Case study 001 - public WFC3/IR data

Diagnosing a hidden ramp transient in WFC3/IR HgCdTe data

Why spatial inspection alone would accept affected reads - and bias the final count-rate product.

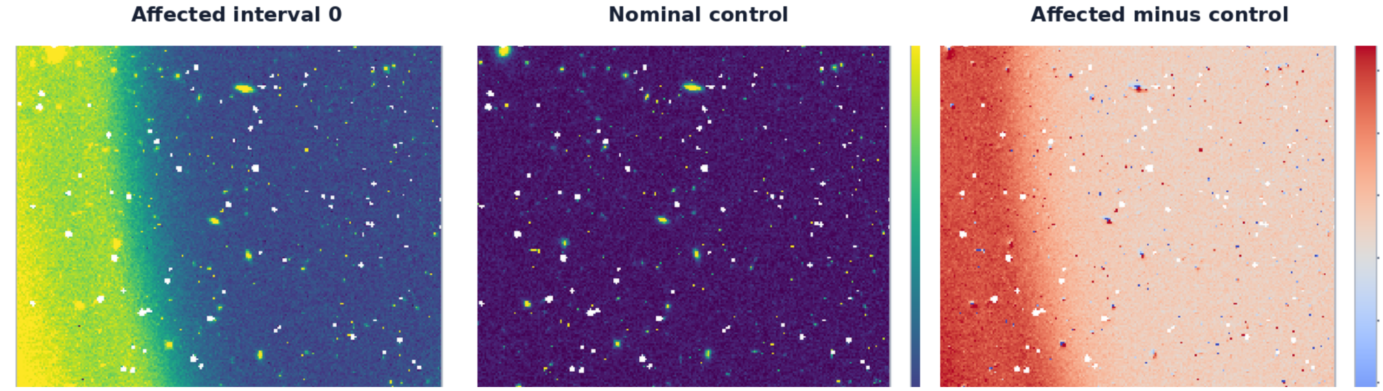

0 to 3
Spatially anomalous intervals

0 to 6
Common-mode intervals

700 s
Transient duration

16.1%
Excess relative to nominal charge

> The strong spatial gradient disappears while the control-relative transient persists. A spatial-only diagnostic would stop three intervals too early.

Analysis by Brooks Photonics using public HST WFC3/IR measurements from MAST.
No client data are represented.

BP-CS-001-T
Rev 1.7 · 2026-08-01

Finding and method

Read-level evidence identifies a time-variable external background

Intervals **0 to 3** contain pronounced left-right structure. A lower-amplitude detector-wide excess remains through interval **6**, producing a total transient duration of **700 s**. No intrinsic detector-material explanation is required by the data.

Supported mechanism: time-variable external background

The effect decays within one exposure, is absent from the matched control, survives source masking, and changes the reconstructed slope.

Reconstruct charge
Recover cumulative charge from calibrated reads.

Measure intervals
Calculate consecutive-read rates.

Separate modes
Evaluate spatial and common-mode behavior independently.

Refit the ramp
Exclude the transient and compare the result.

53.85%
Peak affected asymmetry
1.83% in the nominal control.

0.4958
Peak excess rate
electrons s^{-1} $pixel^{-1}$ after control and offset correction.

94.25%
Source-free pixels retained
Classification agreement remains 100%.

2,000
Bootstrap replicates
All retain the nominal 700 s duration.

Relevance to detector development and production

- Detect time-dependent artifacts hidden by final fitted outputs.
- Separate device nonuniformity from common-mode test conditions.
- Quantify decision sensitivity and uncertainty.
- Specify the minimum additional measurement needed to resolve ambiguity.

Source distinction. STScI documents the affected/control exposure pair, the Earth-limb scattered-light interpretation, and the read-level visualization example. Brooks Photonics independently adds spatial-versus-common-mode endpoint separation, source-mask and threshold sensitivity tests, block-bootstrap uncertainty, and quantitative post-transient refitting.

Spatial evolution

The gradient collapses first; the common-mode tail remains

Three decision-relevant stages show the transition from an obvious spatial anomaly to a temporally elevated but visually subtle detector state.

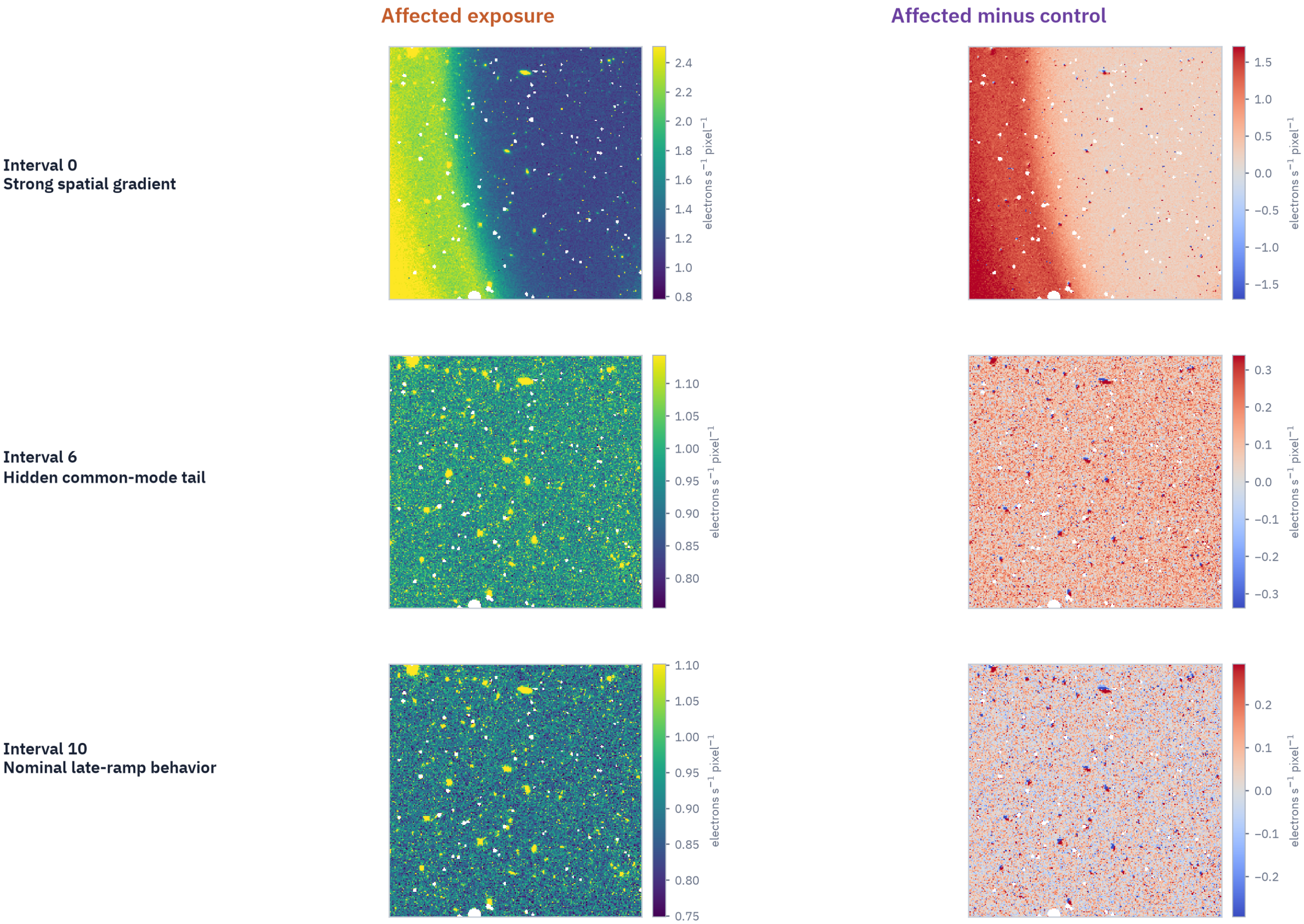

Figure 1. Affected exposure and affected-minus-control maps for intervals 0, 6, and 10. The map scales remain interval-specific to preserve spatial detail; quantitative acceptance is determined from the temporal analysis on the next page.

Temporal diagnosis and robustness

Three affected intervals remain after visual stabilization

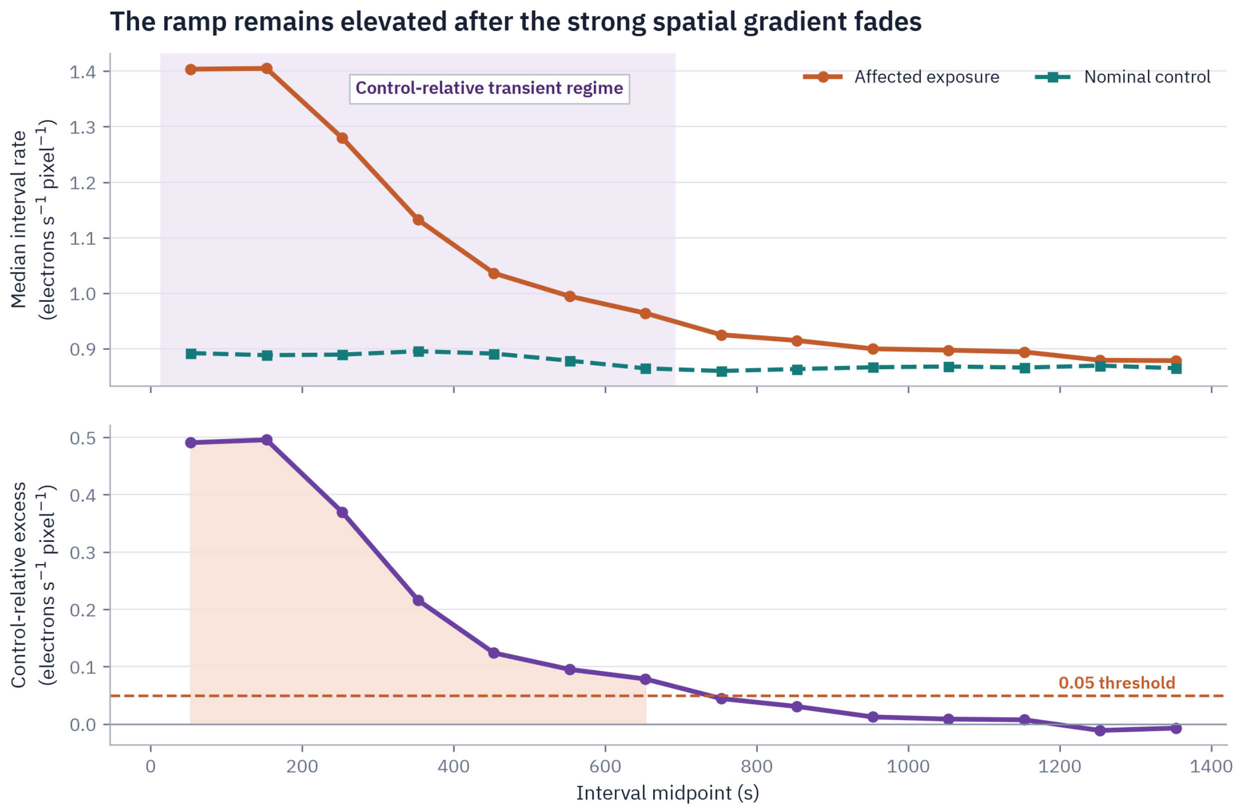

Figure 2. Intervals 0 to 6 exceed the nominal 0.05 electrons s^{-1} pixel^{-1} limit after matched-control subtraction and late-offset removal. The limit is 4.28 times the robust late-ramp residual scale (0.01167 electrons s^{-1} pixel^{-1}) and is not an official WFC3 pipeline threshold.

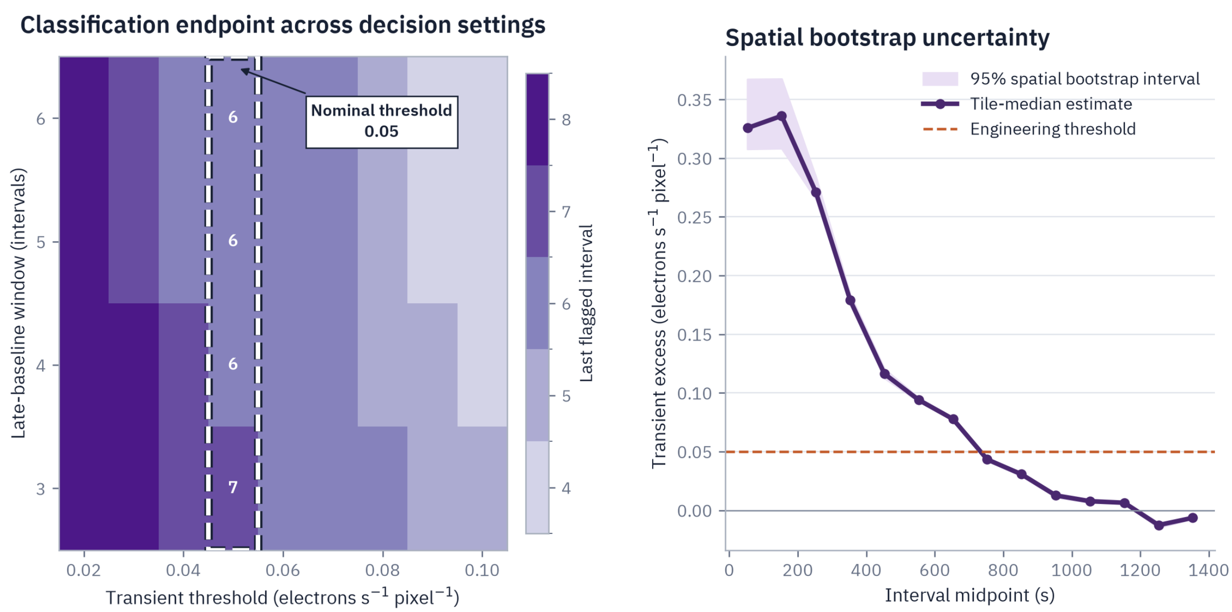

Figure 3. The decision endpoint is stable across threshold and late-baseline choices. Spatial block resampling preserves the 700 s classification duration.

Estimator distinction. The detector-wide median gives 197.26 electrons pixel^{-1}; the spatially robust tile-median gives 150.03 electrons pixel^{-1}. These are different estimands, not competing estimates of one quantity.

Independent reconstruction

Excluding the transient changes the inferred count-rate product

A free-intercept, DQ-aware ordinary-least-squares fit begins at **702.934 s**, after interval 6. Early excess charge is then absorbed by the intercept rather than forcing the later slope upward.

Archived and independently reconstructed count-rate products

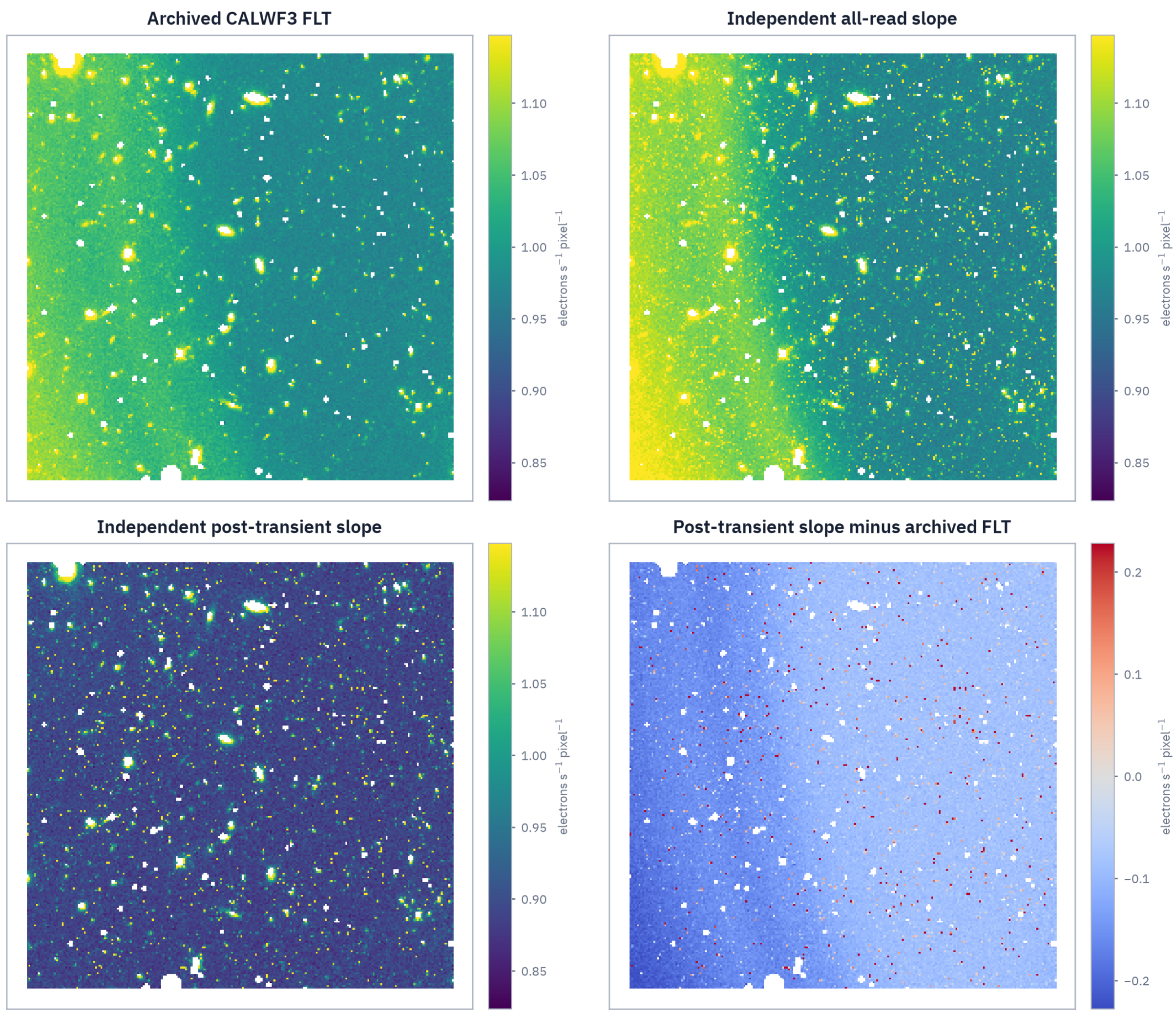

Figure 4. Archived CALWF3 FLT, independent all-read slope, independent post-transient slope, and post-transient-minus-FLT residual.

6.32% to 0.40%
Left-right asymmetry after transient exclusion

0.11108
Lower than archived FLT in electrons s^{-1} pixel^{-1}

PRODUCT OR FIT	SOURCE-FREE MEDIAN	LEFT-RIGHT ASYMMETRY
Archived CALWF3 FLT	1.00296 electrons s^{-1} pixel^{-1}	6.32%
Independent all-read fit	0.99992 electrons s^{-1} pixel^{-1}	9.55%
Independent post-transient fit	0.89337 electrons s^{-1} pixel^{-1}	0.40%

Engineering disposition

Test temporal and spatial integrity separately

1. **Inspect consecutive-read maps**
   Do not accept a final slope product without interval-level review.
2. **Classify spatial and common-mode effects independently**
   A detector can appear uniform while retaining a measurable temporal background.
3. **Use a matched control or validated late baseline**
   Separate static offsets from decaying transients before thresholding.
4. **Quantify decision sensitivity**
   Report threshold, baseline, source-mask, and spatial-resampling dependence.
5. **Refit after transient exclusion**
   Compare slope, residual structure, and operational metrics with the production result.

Evidence-rating standard

Supported	Consistent with all principal observations.
Plausible secondary	May contribute, but cannot explain the full result.
Disfavored	Conflicts with one or more major observations.
Not evaluated	Insufficient evidence in the available data.

MECHANISM	ASSESSMENT
Time-variable external background	**Supported** Temporal decay, spatial evolution, and control comparison agree.
Readout-quadrant offset	**Plausible secondary** May contribute, but cannot explain the smooth detector-wide decay.
Stable gain or flat-field nonuniformity	**Disfavored** Expected to persist and appear similarly in the control.
Intrinsic dark-current nonuniformity	**Disfavored** The pattern decays within one exposure.
Isolated cosmic-ray event	**Disfavored** Cannot explain detector-wide smooth decay.

Data provenance

Four pinned MAST products are verified by byte count and SHA-256. Raw FITS files remain outside Git; the repository stores exact URIs, derived tables, figures, tests, and the complete execution workflow. Open the repository and reproducibility package.

Primary references

[1] O'Connor, A., Khandrika, H., Mack, J., and Calamida, A. (2023), *WFC3/IR IMA Visualization Tools with an Example of Time Variable Background*, HST/WFC3 Notebooks, updated 2023-05-05.

[2] Pagul, A., Rivera, I., et al. (2024), *WFC3 Data Handbook*, Version 6.0, Space Telescope Science Institute.

[3] Mikulski Archive for Space Telescopes (MAST), HST public product archive and download API; products retrieved for Case 001 in 2026.

Interpretation boundary. This case does not infer HgCdTe composition, carrier lifetime, dark-current mechanism, responsivity, detectivity, or intrinsic material quality. The 0.05 electrons s^{-1} $pixel^{-1}$ threshold was selected before the sensitivity sweep at 4.28 times the robust late-ramp residual scale (0.01167 electrons s^{-1} $pixel^{-1}$). It is a transparent engineering operating limit, not an official WFC3 pipeline threshold.

Appendix A - Method and DQ policy

The analysis preserves read-level evidence that final ramp fitting can conceal

Each IMA extension is sorted into chronological order. Cumulative charge is reconstructed before consecutive-read rates are calculated, ensuring that the diagnostic operates on the physical increment between reads rather than on the final fitted slope alone.

Charge reconstruction

$$Q_i(x,y) = R_i(x,y)t_i$$

Consecutive-read interval rate

$$q_i(x,y) = [Q_i(x,y) - Q_{i-1}(x,y)] / [t_i - t_{i-1}]$$

Data-quality policy

Every standard 16-bit WFC3 DQ flag is rejected except **DATAREJECT = 8192**. DATAREJECT is generated by the up-the-ramp fit and is retained as diagnostic evidence rather than treated as a permanent detector defect.

35.80% of affected-array pixels carry DATAREJECT in at least one read.

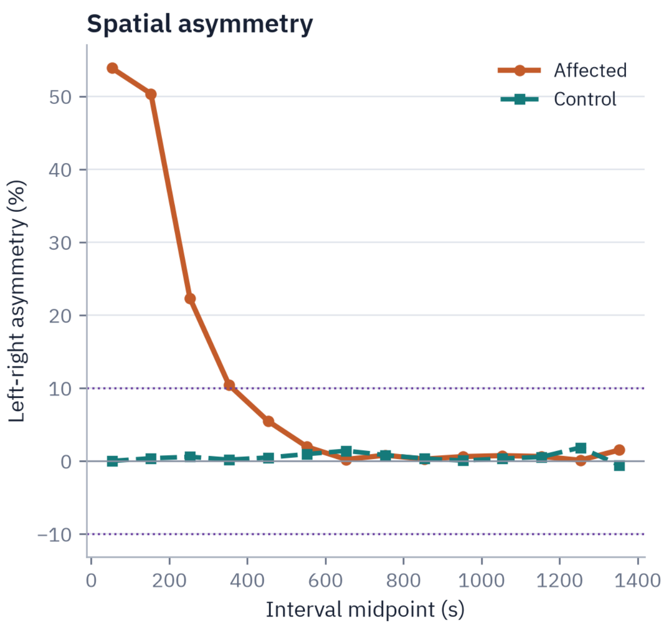

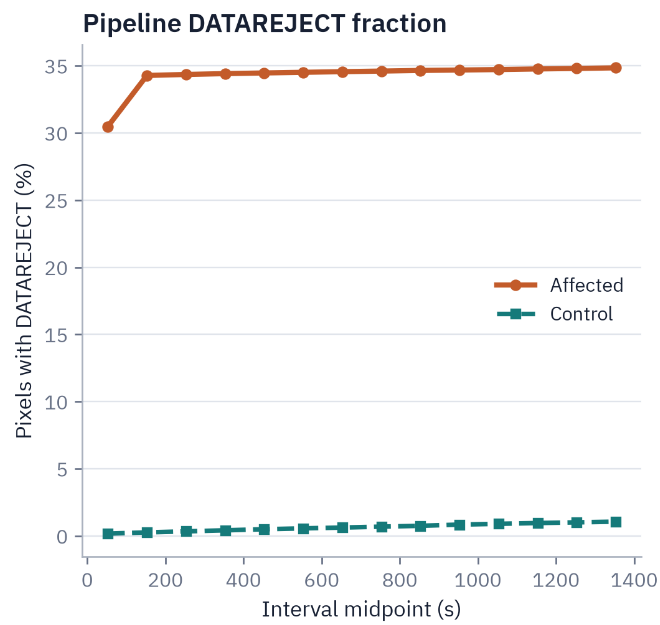

Figure A1. Spatial asymmetry and the pipeline DATAREJECT response evolve together. Affected and control data are encoded by color, marker, and line style.

ANALYSIS COMPONENT	IMPLEMENTATION
Spatial statistic	Sigma-clipped full-frame, left-half, and right-half medians
Common-mode comparison	Matched-control subtraction with late-ramp static-offset correction
Source rejection	Late-control source mask with morphological dilation
Uncertainty	779 spatial tiles and 2,000 block-bootstrap replicates
Independent reconstruction	Free-intercept DQ-aware ordinary-least-squares ramp slope

Appendix B - Complete spatial sequence

The complete interval sequence documents the transition from gradient to common mode

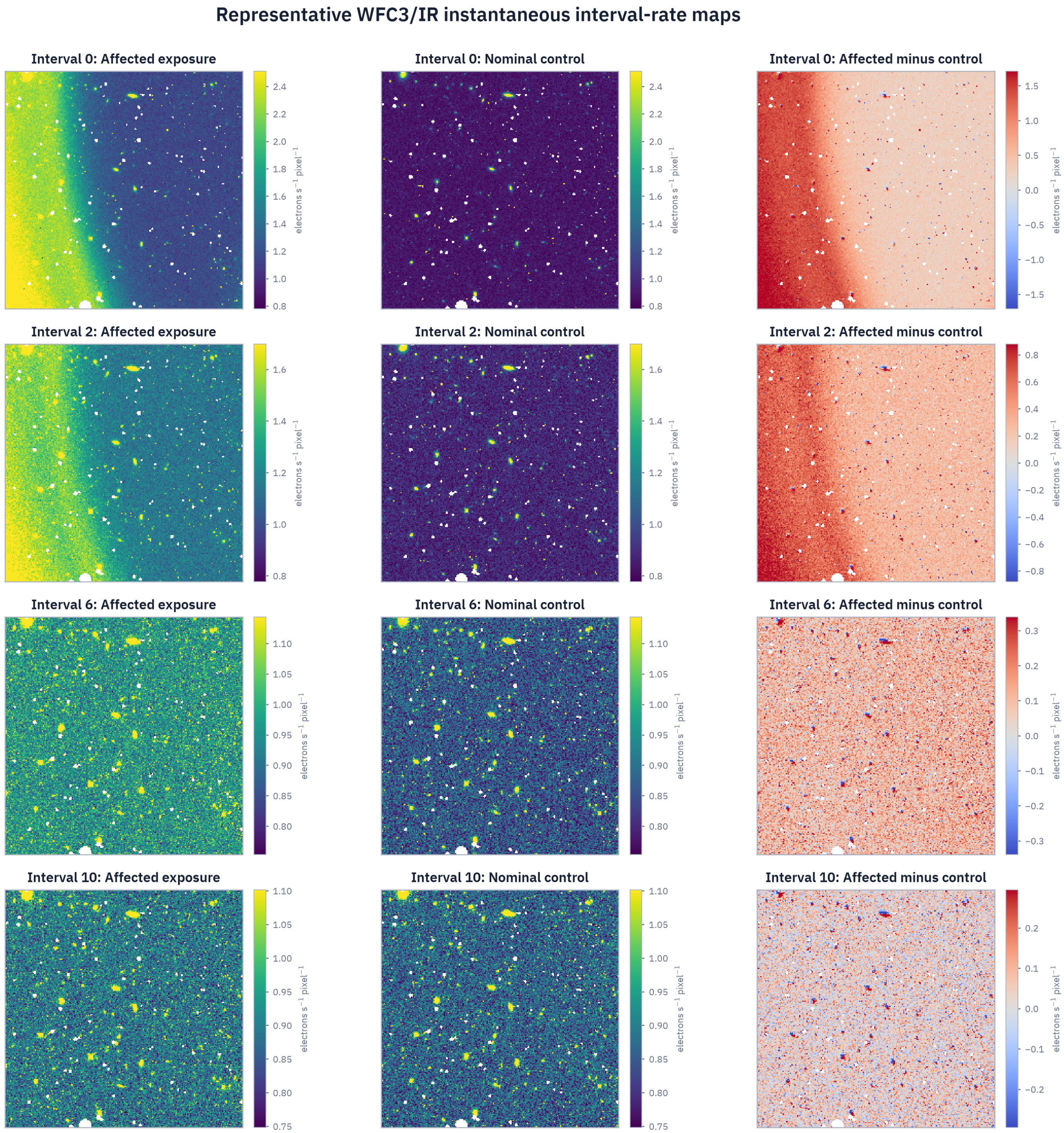

Figure B1. Affected exposure, nominal control, and matched difference at intervals 0, 2, 6, and 10. Interval-specific color scales preserve late-stage spatial detail; absolute acceptance is based on the temporal statistics reported in Figure 2.

Appendix C - Provenance and reproducibility

Every source product and derived result is traceable

The complete case can be regenerated from four pinned public products. Open the source repository. The workflow verifies source files, executes the analysis, runs lint and unit tests, builds both reports, and publishes the derived package as a GitHub Actions artifact.

PRODUCT	BYTES	SHA-256
icqtbbbxq_ima.fits	168,261,120	7b8ff356c5c00a35e2576f2c81dc14ebb1c735f0cee343918b8bbf4f26494a0c
icqtbbc0q_ima.fits	168,261,120	4d9db90cdb11f2c7934c412c02102528d9d184711081e706733d3b37280fd9b5
icqtbbbxq_flt.fits	16,583,040	8b848b19ffac43857b413a2513e97194ea3a17a4899cb09292f293912c11c9d5
icqtbbc0q_flt.fits	16,583,040	21b2876584378b9ccaa6fcc012c2a724d26f4a4c87aa68df74a5d52719824ace

Primary derived products

case_summary.json	Top-level quantified findings
exposure_comparison.csv	Interval-level matched comparison
threshold_sensitivity.csv	Decision robustness sweep
bootstrap_interval_uncertainty.csv	Spatial uncertainty intervals
flt_reconstruction_metrics.json	Archived versus independent fit comparison

Execution record

Repository commit	cb6e1ff3c151
Document identifier	BP-CS-001-T
Report revision	Rev 1.7
Build date	2026-08-01 UTC
Workflow run	30698796956
Python package	brooks-photonics-cases 0.1.0
Client report	Six pages
Technical report	Nine pages
Validation	Ruff, Pytest, product verification

References

[1] O’Connor, A., Khandrika, H., Mack, J., and Calamida, A. (2023). *WFC3/IR IMA Visualization Tools with an Example of Time Variable Background*. HST/WFC3 Notebooks; updated 2023-05-05.

[2] O’Connor, A., Mack, J., Calamida, A., and Khandrika, H. (2023). *Correcting for Scattered Light in WFC3/IR Exposures: Manually Subtracting Bad Reads*. HST/WFC3 Notebooks; updated 2023-11-13.

[3] Pagul, A., Rivera, I., et al. (2024). *WFC3 Data Handbook*, Version 6.0. Baltimore: Space Telescope Science Institute.

[4] Marinelli, M., and Green, J. (2025). *Wide Field Camera 3 Instrument Handbook*, Version 18.0. Baltimore: Space Telescope Science Institute.

[5] Mikulski Archive for Space Telescopes (MAST). HST public product archive and download API; products and persistent product identifiers listed in the provenance table.

Source and reproducibility package

Source code pinned to cb6e1ff3c151, with the product manifest, derived tables, figures, tests, and report workflow.

Brooks Photonics | brooks-photonics.com | terence@brooks-photonics.com

Interpretation boundary. The 0.05 electrons s^{-1} $pixel^{-1}$ threshold is a transparent engineering criterion, not an official WFC3 pipeline threshold. This case does not infer intrinsic HgCdTe material parameters.